Received: 4 February 2022 | Revised: 27 April 2022 | Accepted: 23 May 2022

IET Microwaves, Antennas & Propagation

DOI: 10.1049/mia2.12269

ORIGINAL RESEARCH

Designing UHF RFID tag antennas with Barcode shape for dual-technology identification

Konstantinos Zannas[1] | Francesco P. Chietera[2] | Abanob Abdelnour[1] | Darine Kaddour[1] | Riccardo Colella[2,3] | Luca Catarinucci[2,3] | Yvan Duroc[4] | Smail Tedjini[1]

[1]University Grenoble Alpes, LCIS Lab, Valence, France

[2]Department of Innovation Engineering, University of Salento, Lecce, Italy

[3]CNIT, National Interuniversity Center for Telecommunications, Lecce, Italy

[4]University Lyon, Université Claude Bernard Lyon 1, INSA Lyon, Ecole Centrale de Lyon, CNRS, UMR5505, Villeurbanne, France

Correspondence

Riccardo Colella, Department of Innovation Engineering, University of Salento, Via Monteroni, 73100 Lecce, Italy.
Email: riccardo.colella@unisalento.it

Abstract

In this paper, a novel methodology to design Ultra High Frequency Radio-Frequency IDentification (UHF RFID) tag antennas with Barcode layout is proposed with the challenging goal of "fusing" both technologies in a single device. Specifically, after a brief recall of the well-known barcode standard, a procedure to design meandered barcode-shaped UHF RFID tags is introduced and discussed leveraging on electromagnetic evidence. The main steps of the proposed method are described by highlighting the constraints inherited by both the adopted technologies, as well as the useful opportunities to automatise the entire antenna design process after a preliminary simulation campaign through a full-wave simulator. Different RFID-Barcode tag antennas are designed, manufactured, and characterised in terms of maximum reading range and tag sensitivity. Obtained results demonstrate the validity of the proposed approach.

KEYWORDS

AK-tag, antenna design, barcodes, dual technology, UHF RFID

1 | INTRODUCTION

The capability of designing passive Ultra High Frequency Radio-Frequency IDentification (UHF RFID) tags in addition to the availability of more and more performing RFID chips is contributing to the capillary diffusion of the RFID technology, with more and more interest from both academia and industry, and widespread applications in the most disparate sectors [1–7].

On the other hand, Barcode technology is expected to be used for the years to come, due to its low cost, pervasive diffusion, and already installed infrastructures.

The combined use of these two technologies has been already tested in several applications [8–10], even if all cases, the RFID and barcode have simply coexisted, serving each one as a back-up/complementary for the other.

Hybrid solutions exploiting both RF and optical identification technologies are also available in the literature. A Quick Response (QR) code/chipless RFID system working in the 3–10 GHz frequency band is proposed in Ref.[11] and a QR code/RFID tag working at 2.45 GHz is presented in Ref.[12]. Nevertheless, such solutions do not lie on standardized RFID technologies.

A step forward towards the fusion of the two technologies is presented in Ref.[13], where a preliminary proof of concept regarding the transformation of RFID tags to Barcode structures on standard substrates is studied and experimentally validated. The idea is to have in a single device a well-working RFID tag antenna purposely shaped as a barcode to enable a true dual-technology identification. It should be noted that there are some commercial solutions which seem to serve the same proposed functionality, for example, Ref.[14]. However, in these solutions the two functions co-exist but they are performed independently. In the proposed solution, the barcode pattern plays not only the double role of barcode (by definition), but also of UHF RFID tag antenna. This "hardware" coupling and fusion between the two pieces of information, RFID and Barcode, in a single device can be exploited to secure the tag and could be used to perform authentication functions. The information stored in RFID chip and the information in the barcode structure can be combined to generate a specific ID code to authenticate the device. Indeed, different from the common case in which the barcode is printed on a paper label and the RFID tag is attached under the label as a separate "hardware", in this case the correct operation of one of the technologies is intrinsically linked to the correct operation of the other. In other words, the device is unique and there is no possibility to separate an element (e.g., barcode) from the other, without damaging the whole device. Therefore, if one of the two information blocks is corrupted the authentication fails. Of course, this approach could be better accomplished by using a dual-technology reader.

In this work, the procedure to turn Barcodes into RFID tag antennas is explored in more depth, aiming at deriving an algorithm allowing the automatic generation of well-performing RFID-Barcode antennas, with adequate robustness to the "code" variation. A systematic design procedure is proposed, laying on the transformation of an ordinary Barcode to a working meander dipole tag antenna.

The logic behind the proposed design strategy is discussed, always taking into consideration the constraints imposed by a complexity of developing antenna structures. At this regard, some possible solutions to the problem of realizing antennas with different shapes and sizes that need to properly work at the same frequency (which is 865–867 MHz for the European Telecommunications Standards Institute [ETSI] band) are addressed. To validate these considerations, several RFID-Barcode tags are realised on a thin paper substrate as proof, while their performances are evaluated in terms of read range and tag sensitivity both with a commercial [15] and lab-made characterisation systems [16], in order to verify the aptness of the introduced procedure.

2 | BARCODE-SHAPE RFID TAG ANTENNA DESIGN

In this paragraph a procedure to design working UHF RFID tag antennas starting from a barcode layout is introduced. Specifically, the Barcode protocols are firstly introduced and the main elements exploitable to design a dual-technology device are highlighted. Then, the procedure to automatically obtain a working Barcode-Tag is described.

2.1 | From Barcode to antenna

Currently, there are several Barcode protocols compliant to the GS1 global standard [17] like EAN-8, EAN-13, GS1-128, UPC-A and UPC-C. However, all the protocols share the same main structure: a series of bars with different width and spacing depending on the specific code. In this work the GS1-128 protocol, whose structure is shown in Figure 1, is considered without loss of generality. Observed through the eyes of an expert of electromagnetics, the structure of Figure 1 could be roughly associated to that of a meandered dipole antenna, with the difference that the vertical bars are not properly interconnected together.

FIGURE 1 Example of GS1-128 Barcode structure

However, to understand which elements of the barcode structure are constraints and which can be modified in the process of the antenna generation, a brief overview on the GS1-128 symbology is mandatory. Specifically, it is composed by 5 sections: the Start Character (Start A, B or C); the Function Code 1 (FNC1); the Data; a Check Symbol Character; the End Character.

The maximum length of the total Barcode is 165 mm including the so-called Quiet Zones. There are two Quiet Zones (see Figure 1), positioned just before the Start Character and just after the End Character, respectively. The two zones are compulsory for reading the Barcode. The width of each Quite Zone should be 10 times the minimum width used for the representation of a character's element. The minimum width of the Barcode can be 15% of its length.

The Start Character can either be the character A, B or C. Each character option specifies the usage of the respective code sets A, B or C. These GS1-128 code sets are available in Ref.[18]. The FNC1 is always used in order to be identified as a GS1 standard and it is placed immediately after the start character. The data part follows the FNC1 character. The maximum number of data characters is 48. The Check Symbol is used immediately after the data, and it is not shown in the Human Readable Interpretation. The Check Symbol is calculated by a weighted function of the Start Character, the FNC1 and the data characters. Finally, the End Character is always at the end of the Barcode, and it is unique since it is composed from 4 black (commonly bars) and 3 white (commonly spaces) modules. All the other characters are composed by 3 black and 3 white modules.

In Figure 2 an example of Barcode coding referred to the word FRIT is presented. As can be seen, every character is composed by 11 elements, except the End Character which consists of 13 elements. The width of each element in a single Barcode is fixed. In general, it can vary between 0.250 and 1.016 mm.

Based on these constraints, several operations could be performed with the goal of transforming a generic Barcode

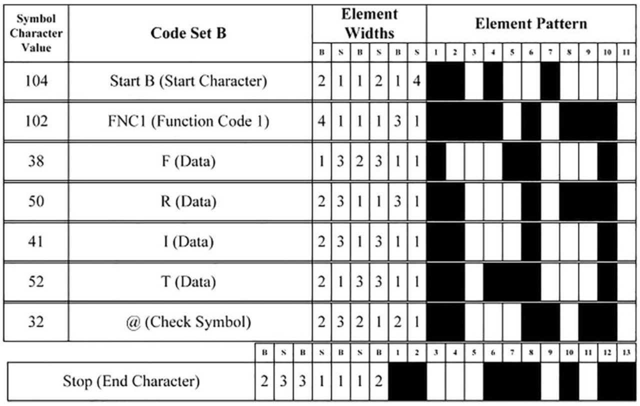

FIGURE 2 Example of the GS1-128 representation of the word "FRIT"

structure in a UHF meandered antenna properly useable as an RFID tag. This conversion is mainly performed by connecting opportunely some of the black "bars" so obtaining a sort of meandered shape, which is quite similar to a standard UHF RFID dipole antenna. However, the variable length of the encoded message needs to be faced up so to tune the working frequency of the antenna that has to remain stable around 866 MHz in ETSI band. To do so, after setting an initial length of the dipole and a minimum width of the bars as starting point, the height of the bars can be tuned for the scope. On the other hand, if a too long message is encoded in the barcode, so determining a too long dipole, some of the barcode parts can be left apart from the connection, so shortening the effective electrical length of the antenna.

A statistical analysis on the effect of these tuning strategies on the behaviour of a generic RFID-Barcode tag when the message length varies can be performed. This could enable a sort of automated decision process based on full-wave simulations, and fast enough to be easily integrated into a large-scale production process.

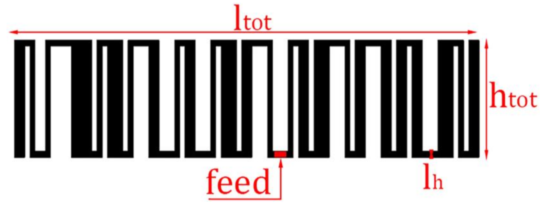

FIGURE 3 Tuning parameters of a Barcode-shaped Ultra High Frequency Radio-Frequency IDentification tag antenna: direct feeder

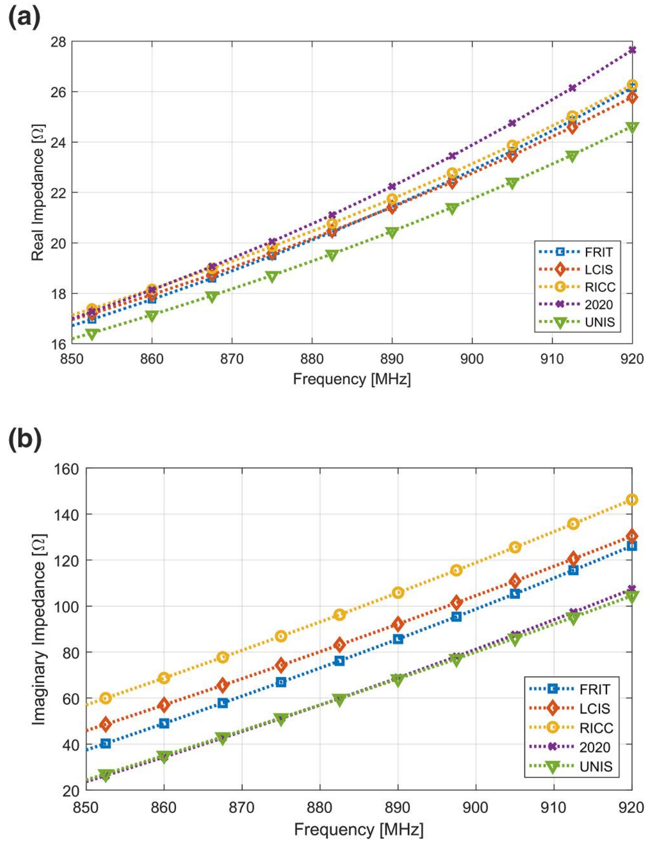

FIGURE 4 Comparison among the Real part (a) and Imaginary part (b) of the impedances for a selection of barcode-derived antennas

2.2 | Barcode-tag design procedure

As stated in the previous sub-section, the realisation of dual-technology devices allows the retrieving of the ID code through both optical and RFID readers due to the similarity between a generic barcode and a meander antenna.

The first attempts published in Ref.[13] demonstrated how it is definitely possible, given a specific barcode, to work on its electromagnetic design by acting on the number of connected bars and size to ensure a proper functioning, not only as a barcode but also as an RFID tag. However, it is evident how it is impractical to design a different antenna for each individual barcode. To be fully useable, in fact, each dual-technology tag, regardless of the specific code, should be printable "on-demand" without any ad hoc electromagnetic design.

To make this possible, a specific procedure is necessary, which requires a preliminary step aimed at verifying the sensitivity of the impedance of the antenna derived from the barcode when varying the code itself. The procedure consists of generating in a random way a statistically significant number of codes and to realise the associated bitmap of the barcodes. By means of a specific MATLAB® script, each bitmap image is processed and transformed into a barcode-derived meander antenna, which is realised by connecting alternatively the vertical bars. The feed is automatically set by creating a gap acting as an electrical port for the impedance estimation, as sketched in Figure 3. By exploiting the MATLAB® antenna toolbox, the impedance is evaluated at the frequency of interest of 866 MHz, and the comparison performed.

In Figure 4, for instance, the impedance of a short selection of barcode-derived antennas obtained from 4-char barcodes is reported. It can be observed that the real part is substantially not affected by the code variation, while a slight impact on the imaginary part is observed. More specifically, after an automatised test performed on several randomly generated 4-char codes, a variance of 5% on the real part and 23% on the imaginary part is obtained.

Similar results have been obtained also when comparing barcode-derived antennas starting from longer or shorter codes.

These encouraging results suggest that once a specific barcode tag has been optimised (in terms of height, length, track thickness, number of horizontally connected bars, etc.) to work correctly, a barcode-tag derived from a different code but realised by adopting the same design parameters, will likely work fine as well. Furthermore, since a different code mainly generates a variation on the imaginary part of the antenna impedance, the identification of a parameter acting mainly on the reactance could allow a simple tuning and guarantee even more adequate performance.

In this regard, Figure 3 shows the main tuning parameters to act on so to optimise the barcode-derived antenna, keeping in mind that when the total length l_{tot} is varied, the proportion between size of the bars and their mutual distance must be kept constant since it impacts on the optical readability. An interesting parameter is the thickness of the horizontal bands l_h used to join the vertical bands so as to create the meanders. It is an easily adjustable parameter since it does not affect neither the optical readability nor the size of the tag, which is expected to remain constant when varying the code. Figure 5 shows the results of a parametric analysis performed, without loss of generality, on a barcode-derived antenna referred to as a 4-char code when varying l_h from 0.5 to 3 mm. Despite a negligible impact on the real part of the impedance, an average reactance variation of 15 Ω is observed for each 0.5 mm step. This correlation makes the l_h parameter particularly suitable for and automatised antenna impedance matching procedure.

In summary, all the aforementioned considerations pave the way to the implementation of a specific algorithm which consists of the following steps, also summarised in Figure 6.

1) The desired barcode protocol is selected among those reported in Ref.[17] along with the number of chars of the codes to be generated, on the basis of the specific needs.

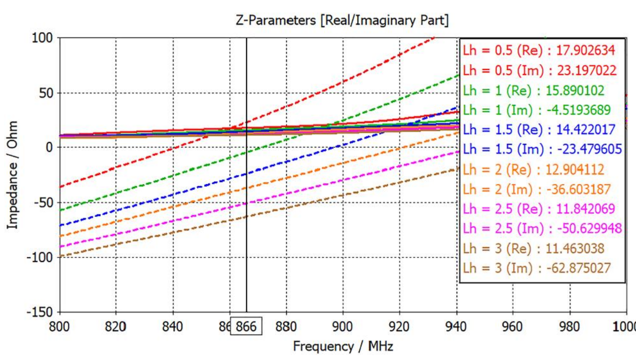

FIGURE 5 Parametric analysis of the impedance of a 4-char barcode-derived antenna when varying the parameter l_h

2) Desired maximum length and height of the device are given in input together with other data such as RFID chip impedance, substrate permittivity (ε_r) and thickness. In addition to the antenna substrate, the electromagnetic ($\varepsilon_{r\text{-}back}$, σ_{back}) and dimensional characteristics of the background on which the antenna is intended to work (or to better perform) can be set at this stage, to be taken into account in the next steps.
3) A first code is generated.
4) By means of electromagnetic simulations, the parameter l_{tot} is used to determine the bars to be interconnected to form the meanders, and the bars that will not be part of the antenna. The goal is to achieve a resonance as close as possible to the desired working frequency (e.g., 866 MHz for ETSI standard).
5) The related barcode-tag is then optimised by acting on all the individuated tuning parameters (e.g., l_{tot}, h_{tot}, l_h).
6) Optimised values of the tuning parameters are saved.

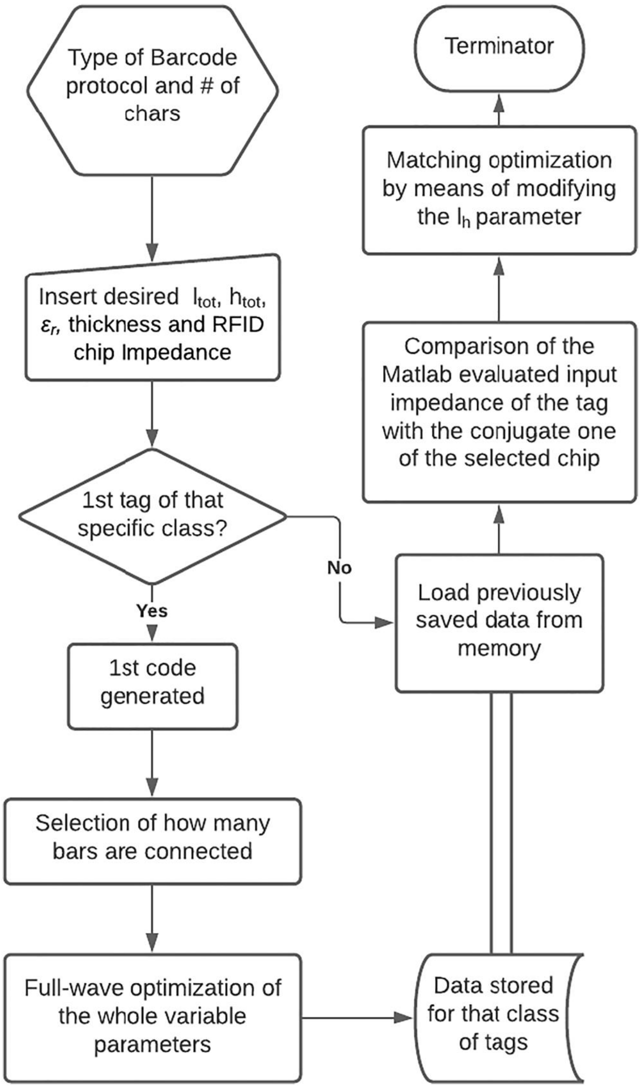

FIGURE 6 Flowchart of the proposed Algorithm for Barcode-shaped Ultra High Frequency Radio-Frequency IDentification tag antennas generation

7) For each further code, the related barcode-tag is straightforwardly generated by using the saved tuning parameters.
8) A rapid check on the antenna input impedance is performed through the MATLAB® antenna toolbox and the obtained reactance is compared with one of the conjugate impedances of the RFID chip.
9) If possible, the matching quality is improved by increasing/decreasing, in steps, the size of the horizontal bars (l_h) to achieve the best possible impedance matching, given the constrains. Note that to avoid further "work-in-progress" simulations the average correlation l_h-reactance is preliminarily evaluated for each barcode-family, tabulated, and saved. This makes straightforward the finding of the right l_h value that tunes the reactance and finalises the antenna design.

It is worth highlighting that, in the specific case, the antenna shapes have been parameterised and optimised to reduce the return loss in the considered RFID frequency band using the Surrogate Model Assisted Differential Evolution Algorithm (SADEA) [19]. The SADEA Optimiser has been used to combine the capabilities of CST Microwave Studio® electromagnetic environment, adopted to design the reference barcode-antenna model, with those of MATLAB® environment, used to implement the automatic optimization strategy. In particular, antenna-chip impedance matching and antenna gain have been selected as the final goal of the optimisation by using all the individuated tuning parameters (e.g., l_{tot}, h_{tot}, l_h) as variables.

In order to test the proposed procedure, different barcode-tags have been realised and fully characterised from the electromagnetic point of view. For ease of fabrication, and especially to avoid the soldering of an RFID chip, a coupled Adaptive Kernel (AK) tag is used to inductively feed the RFID-Barcode tag.

The AK-tag is a parallelogram loop antenna with dimensions 11.54 × 9.2 mm equipped with the Impinj Monza 5 RFID chip. It intrinsically presents a read range of around 50 cm. But when it is coupled with an RFID dipole-like antenna, this read range can be enhanced. The input impedance of the Impinj Monza 5 RFID chip can be extracted from the linearised model which is available in Ref.[15]. The linearised model consists of the parallel between a resistor $R_p = 1.8$ kΩ and a capacitor with value of $C_p = 1.070$ pF (including the mounting parasitic effects). For instance, the impedance value of the chip calculated in the RFID ETSI band is $Z_{chip} = 16.24\text{-j}170\ \Omega$. Moreover, the read sensitivity of the RFID chip is $S_{chip} = -17.8$ dBm.

With this in mind, it is worth emphasising that the Step #5 of the algorithm is enriched with one more optimisation parameter, that is, the position of the centre of the AK-Tag with respect to the left and bottom edges of the meandered structure (l_{AK} and h_{AK}) as shown in Figure 7. It is worth emphasising that the AK-tag could be placed either above or below of the antenna, by taking into account the presence of the substrate during the simulation phase. The former approach is used in this work for the sake of an easier graphical representation and validation, even if the latter approach is generally preferable to avoid optical interferences and erroneous optical readings due to the superimposed AK-tag pattern. In the next section some examples of RFID-Barcode tags are designed by using the novel algorithm, properly manufactured, and rigorously characterised from the electromagnetic point of view to validate the whole design procedure.

3 | EXAMPLES OF RFID-BARCODE TAG ANTENNA DESIGN

In this section the validation of the proposed procedure to generate RFID-Barcode antennas is presented.

Frist, the RFID-Barcode antenna representing the 4-char word "FRIT" has been designed to occupy a maximum area of 75 × 15 mm^2, and then optimised to guarantee both optical and RF reading by following the novel algorithm procedure. Specifically, the antenna has been designed by using 35μm-copper as a conductor and paper as a substrate with thickness of 0.15 mm and permittivity $\varepsilon_r = 3.87$. The AK-tag equipped with Monza 5 RFID chip has been used as feeder [20]. As a result, the following antenna parameters have been found: l_{tot} = 72.00 mm (obtained by using all the vertical bars), h_{tot} = 14.80 mm, and l_h = 1 mm. Moreover, the following position of the AK tag has been computed for the specific barcode family l_{AK} = 31.5 mm and h_{AK} = 5 mm. Figure 8 shows the obtained antenna with the related dimensional details and the optimised AK-tag position.

To validate the RFID-Barcode antenna, the equivalent numerical model has been designed and simulated. The feeding port has been connected to the input of the modelled AK-tag placed has shown in Figure 8.

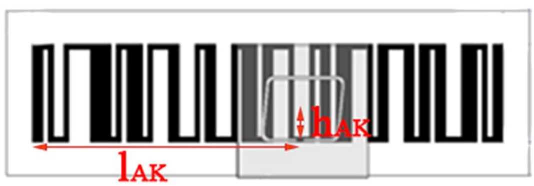

FIGURE 7 Tuning parameters of a Barcode-shaped Ultra High Frequency Radio-Frequency IDentification tag antenna: Adaptive Kernel (AK) tag feeder

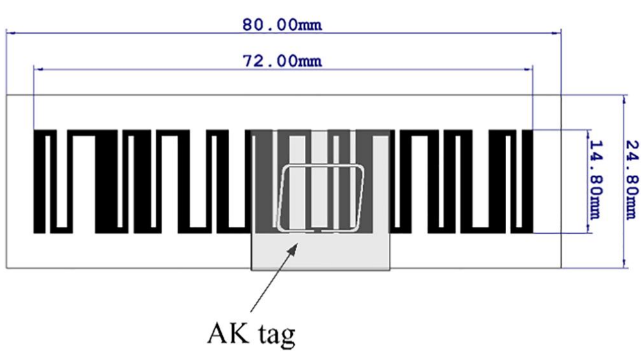

FIGURE 8 Designed RFID-Barcode tag with the position of the AK-tag

In Figure 9 both real and imaginary values of the input impedance of the antenna are presented. The value of the complex input impedance has been found to be $Z_{ant} = 39.2 + j185.6\ \Omega$ at 866 MHz.

In addition, in Figure 10, the simulated radiation pattern of the RFID-Barcode antenna can be found. The maximum gain achieved at 866 MHz is 1.14 dBi. The gain, as expected, has a dipole-like radiation pattern.

To demonstrate the robustness of the proposed procedure two more antennas, representing the same number of characters, were designed with the same dimensional parameters, and positioning AK-tag at the same point coming from the master simulation. The two antennas are presented in Figure 11, corresponding to the words "LCIS" (Figure 11a) and "2020" (Figure 11b), respectively. In addition, to explore cases with more data characters, and generalise the goodness of the used approach, one more RFID-Barcode tag, containing the 10-character code "UNIVLECCE:", has been designed as shown in Figure 12. In this last case, to maintain a reasonable electrical length of the resulting dipole, the antenna has been computed by meandering all the bars except that some of them are placed at the beginning and at the end of the barcode. This is to fulfil the algorithm input requirements, which in this last case have foreseen a maximum total length under 80 mm, and a maximum total height under 15 mm, to guarantee the right barcode proportions to optically read the barcode. This approach is adopted for any number of characters in the Barcode, disconnecting progressively more bars to maintain a correct overall electrical length of the dipole. However, at the end of the automatic design procedure the following parameter values have been obtained for the "UNIVLECCE:" antenna: $l_{tot} = 78.00$ mm, $h_{tot} = 13.20$ mm, $l_b = 0.8$ mm, $l_{AK} = 39.45$ mm, and $h_{AK} = 3.55$ mm.

Finally, all the proposed automatically generated antennas have been manufactured and measured to definitively, and experimentally, validate the procedure, as discussed in the next section.

4 | FABRICATION AND MEASUREMENT OF THE RFID-BARCODE TAG ANTENNAS

The RFID-Barcode tag antennas have been fabricated on a paper substrate of thickness 0.15 mm by precisely shaping an adhesive copper tape of thickness 35 μm through a cutting

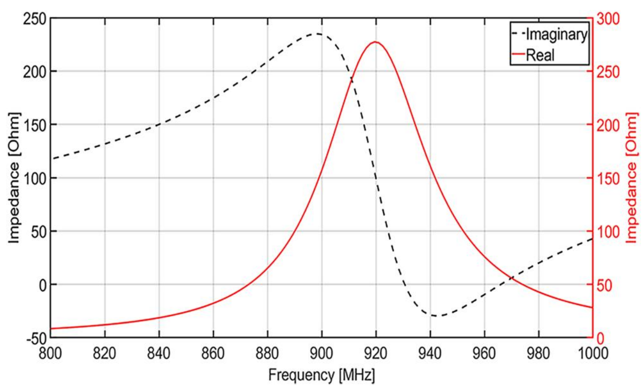

FIGURE 9 Simulated real and imaginary values of input impedance of the "FRIT" RFID-Barcode antenna

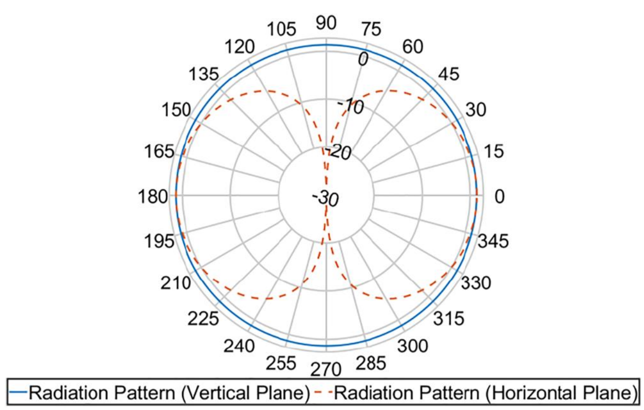

FIGURE 10 Simulated radiation pattern of the RFID-Barcode antenna

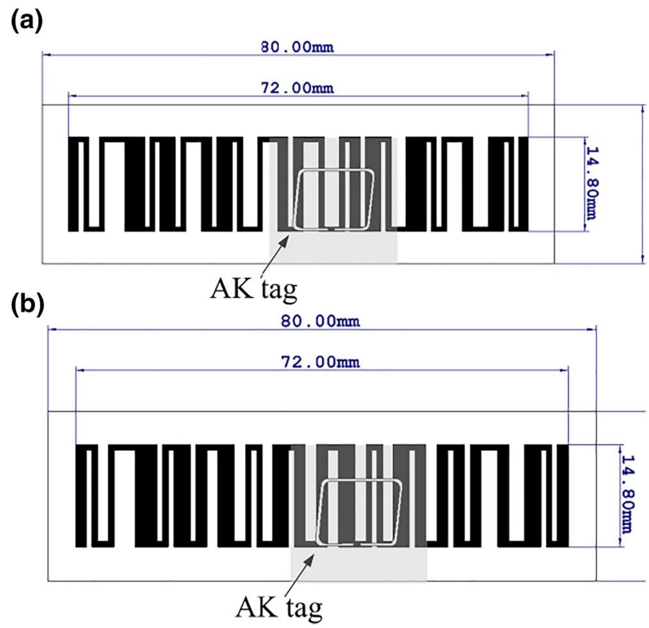

FIGURE 11 Designed RFID-Barcode tags (a) for data "LCIS" (b) for data "2020"

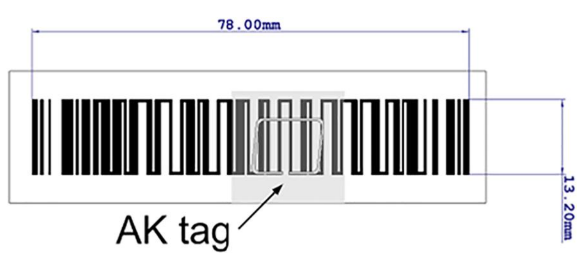

FIGURE 12 Designed RFID-Barcode tag for data "UNIVLECCE"

plotter. Moreover, the AK-tag has been applied on each antenna according to simulation outcomes. As previously stated, for the sake of graphical representation of the realised Barcode-Tags, the AK Tags have been applied on top of the antennas. This means that to correctly read the barcode, the upper side of the antenna has been used.

The fabricated RFID-Barcode tag prototypes are presented in Figure 13 and Figure 14, corresponding to the barcode layouts considering 4 and 10 data characters, respectively.

The RFID-Barcode tags have been characterised both in terms of optical recognition, using a commercial laser barcode reader, as well as in terms of electromagnetic characterisation. As for the optical readability, no missing readings of the barcodes have been observed within a reading distance of 15 cm, regardless of the copper reflectance.

Moreover, as for the characterisation, the most common RFID metrics, which are the estimated maximum reading distance and the tag sensitivity, have been evaluated. The Voyantic Tagformance Pro [15] RFID reader, which is the commercial golden standard for RFID tag characterisation solutions, has been used. Specifically, all the designed RFID barcode-shape tags have been characterised in free-space by pointing the Voyantic Tagformance testing antenna upwards, in the direction of the foam structure supporting the tag under test, as shown in Figure 15a. According to the vendor recommendation, the tag has been placed in front of the testing antenna, in correspondence of the maximum gain direction at the suggested distance of 30 cm. As can be observed in Figure 15b, the testing antenna has been connected to the Voyantic Tagformance through a 50-Ω coaxial cable and an external circulator. This specific hardware configuration is mandatory for performing measurements based on the evaluation of the tag activation power threshold. Indeed, the circulator separates the RF transmit chain from the RF receive chain. The whole equipment has been arranged on a low-permittivity surface and placed at a height of 1.7 m from the ground through wood supports. It has been previously experienced that this height is enough to avoid ground reflections of the retro lobe of the antenna that could affect the measurement. To be sure that the measurement procedure is not affected by the surrounding environment, the system has been initially calibrated through an RFID tag with known RFID chip sensitivity and antenna gain. Then the estimated read range of each RFID-Barcode tag has been measured by gradually increasing the Tagformance output power while measuring the strength of the backscattered signal.

The estimated value inferred through this platform has been compared with the simulated one, obtained through a MATLAB® script implementing the well-known Friis' model

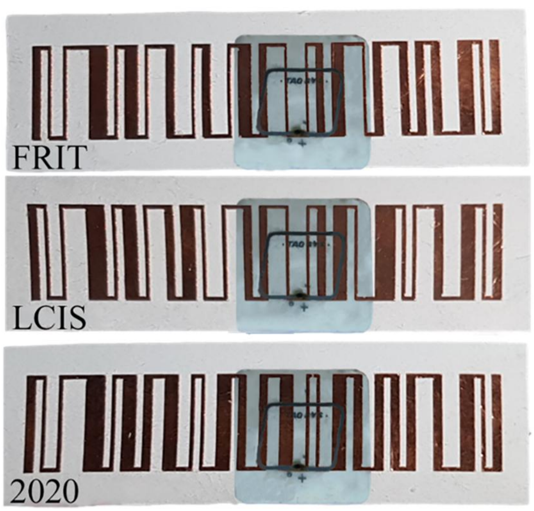

FIGURE 13 Fabricated 4-character RFID-Barcode tags

FIGURE 14 Fabricated 9-character RFID-Barcode tag

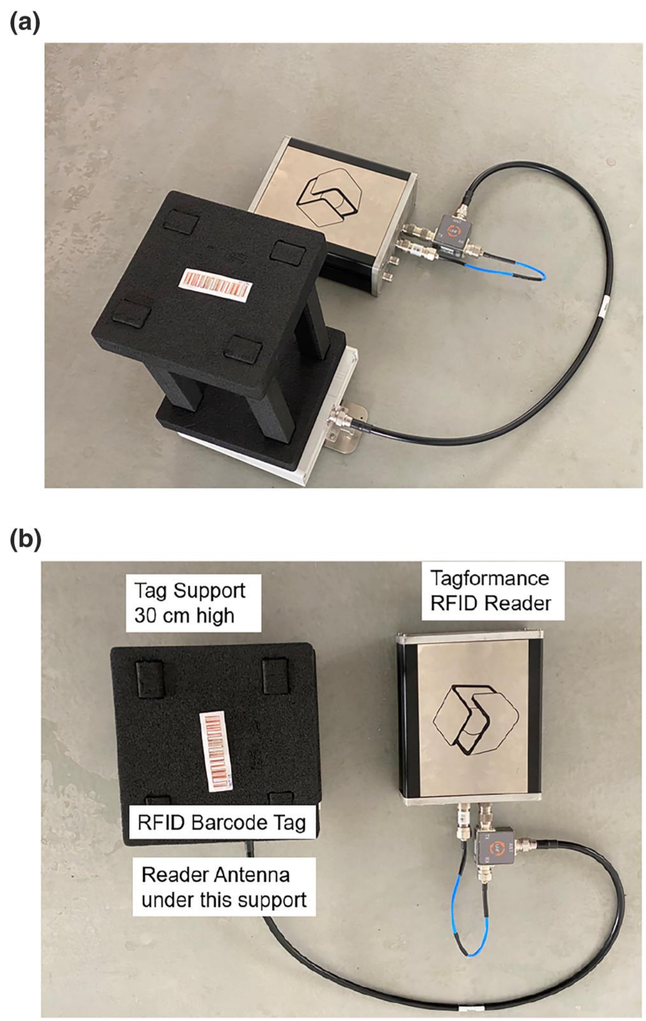

FIGURE 15 Measurement setup for RFID barcode tag characterisation: side view (a) and top view (b)

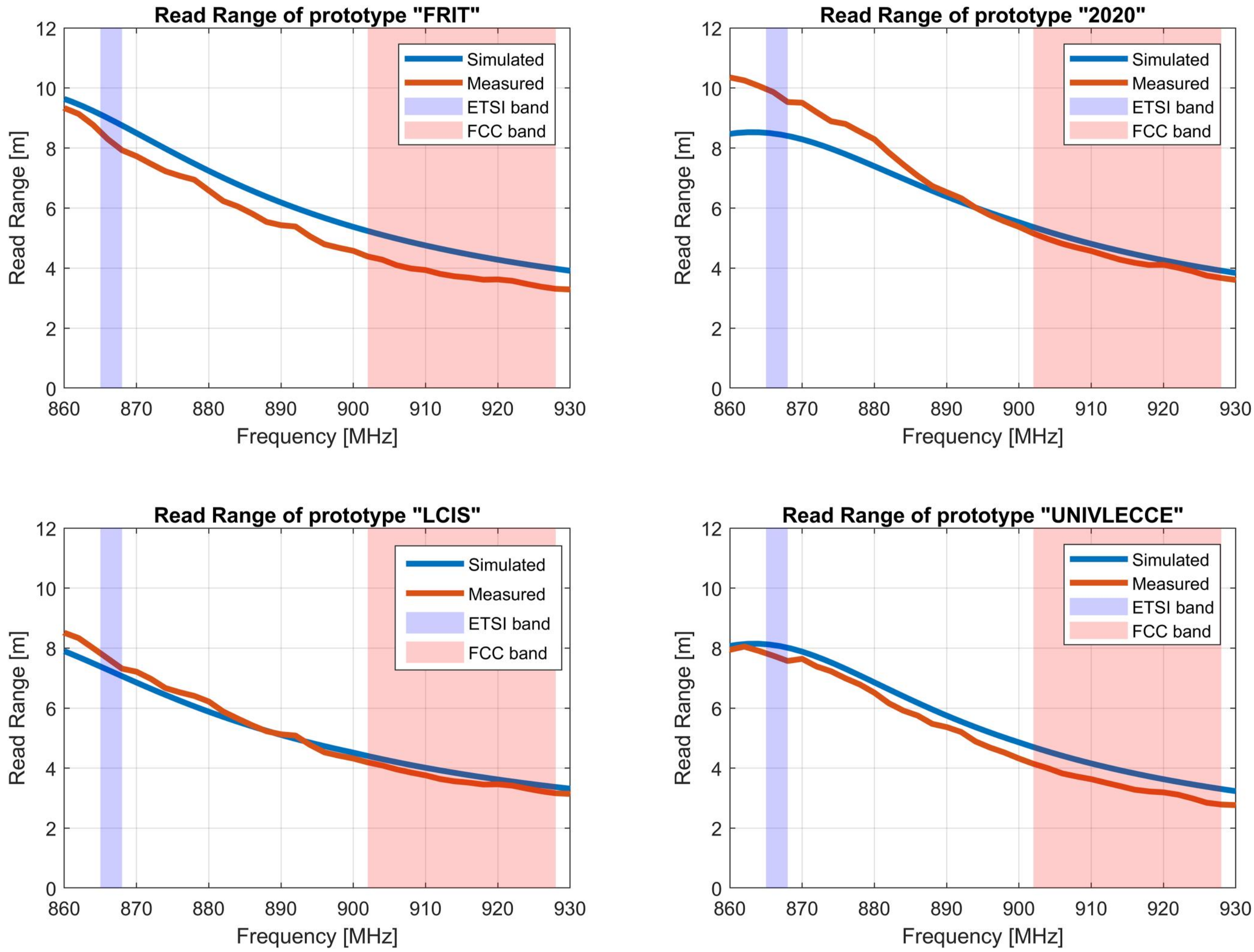

FIGURE 16 Comparison of the measured versus the simulated read range of the fabricated RFID-Barcode tags

of radio propagation in free space specialised for the RFID communications [21]. It takes in input from the simulated transmission coefficient (τ) and the antenna gain, in addition to the declared chip sensitivity, the polarisation loss factor (set to 0.5), and the maximum Effective Isotropic Radiated Powerbe allowed by the European regulation on electromagnetic emissions (which is 35.16 dBm). This comparison is reported in Figure 16 for all the investigated tags. It can be observed how all the realised prototypes ensure appreciable read range (greater than 7 m). This was not obvious at all since the tag shape changes with the different encoded data. Moreover, the behaviour of both simulated and measured curves is similar, even considering acceptable discrepancies (RMSE on the whole RFID band smaller than 0.5 m) due to the RFID chip impedance and sensitivity tolerance and the hand-assisted realisation process. The latter metric, that is, the tag sensitivity, is the minimum RF power at the tag stage capable of activating the RFID chip. It has been measured by using the lab-made characterisation system developed by some of the

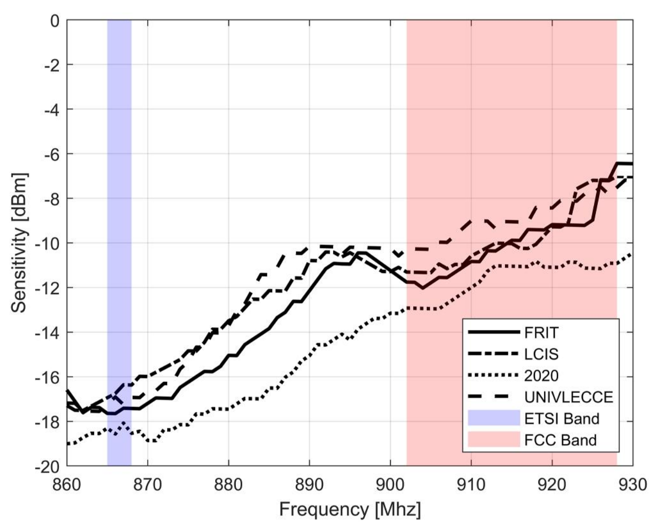

FIGURE 17 Comparison of the measured Sensitivity values of the fabricated RFID-Barcode tags

authors and described in Ref.[16]. The results are reported in Figure 17 where the values related to all the realised prototypes are compared. It emerges how the two measured metrics are in a very good agreement, thus enforcing the goodness of the proposed algorithm for the design of RFID-Barcode tags.

Finally, two extra comments can be done. The first one is referred to the working frequency. Indeed, that the presented RFID-Barcode tags have been designed for ETSI band. It is worth highlighting that, of course, they can be easily adjusted to operate in Federal Communications Commission RFID frequency band. The second one is referred to as a possible large-scale manufacturing procedure. In such a context, the proposed barcode-tag antennas can be easily realised by inkjet printing the RFID-Barcode tags on a paper or on a polyethylene terephthalate substrate with the use of conductive ink. Such a printing technique of RFID tags has been well-demonstrated in a variety of publications [22–25]. This easiness of fabrication, joint with the fastness of the proposed automated procedure for barcode-tags generation, can pave the way to a feasible commercial application of the discussed dual technology.

5 | CONCLUSION

A design methodology for the generation of meandered structures which works properly both as RFID tag antenna and Barcode, for a dual-technology readability, has been proposed. Specifically, an automated process to fast optimise tags which encode different "codes" has been described and tested. It is based on the robustness of the input impedance, properly demonstrated, when varying the code, and on the individuation of some design and tuning parameters which have an impact on the antenna performance without affecting the optical readability.

The procedure foresees two different steps. The former is aimed at evaluating and saving all the main design parameters of a given Barcode family by the means of a full-wave simulation. The latter exploits the saved parameters to generate any other RFID-Barcode Tag of the same family and, optionally, to improve the antenna-chip conjugate impedance matching. It is performed by the means of a rapid evaluation of the antenna input impedance and the consequent selection of proper preset parameters. The algorithm has been used to generate different RFID-Barcode tags, and their optical and RF performance have been evaluated and discussed. While varying the code, all the RFID-Barcode tags assure a reading range higher than 7 m in the ETSI frequency band thus demonstrating the validity of the proposed approach.

ACKNOWLEDGEMENT

The authors would like to thank Rakotomalala Imbolatiana for assisting with the measurement procedure of the fabricated prototypes.

CONFLICT OF INTEREST

No authors have a conflict of interest to disclose.

PERMISSION TO REPRODUCE MATERIALS FROM OTHER SOURCES:

None.

DATA AVAILABILITY STATEMENT

The data that support the findings of this study are available from the corresponding author upon reasonable request.

ORCID

Luca Catarinucci https://orcid.org/0000-0001-9735-6844

REFERENCES

1. Li, X., et al.: UHF RFID tag antenna based on the DLS-EBG structure for metallic objects. IET Microw. Antenn. Propag. 14(7), 567–572 (2020). https://doi.org/10.1049/iet-map.2019.0780
2. Babaeian, F., Karmakar, N.C.: Development of cross-polar orientation-insensitive chipless RFID tags. IEEE Trans. Antenn. Propag. 68(7), 5159–5170 (2020). https://doi.org/10.1109/tap.2020.2975639
3. Catarinucci, L., Colella, R., Tarricone, L.: Sensor data transmission through passive RFID tags to feed wireless sensor networks. In: 2010 IEEE MTT-S International Microwave Symposium, pp. 1772–1775. MTT 2010, Anaheim (2010)
4. Jiang, Y., et al.: e-Textile embroidered wearable near-field communication RFID antennas. IET Microw., Antennas Propag. 13(1), 99–104 (2019). https://doi.org/10.1049/iet-map.2018.5435
5. Colella, R., Catarinucci, L.: Wearable UHF RFID sensor-tag based on customized 3D-printed antenna substrates. IEEE Sensor. J. 18(21), 8789–8795 (2018). https://doi.org/10.1109/jsen.2018.2867597
6. Zannas, K., et al.: A flipping UHF RFID sensor-tag for metallic environment compliant with ETSI/FCC bands. IEEE Trans. Antenn. Propag. 69(3), 1283–1292 (2021). https://doi.org/10.1109/tap.2020.3026869
7. Ripin, N., et al.: Miniature folded dipolar patch with embedded AMC for metal mountable tag design. IEEE Trans. Antenn. Propag. 68(5), 3525–3533 (2020). https://doi.org/10.1109/tap.2020.2969814
8. Mun, I.K., et al.: Active RFID system augmented with 2D barcode for asset management in a hospital setting. In: 2007 IEEE International Conference on RFID, pp. 205–211. Grapevine, TX (2007)
9. Bite, K.E.: Improving on passenger and baggage processes at airports with RFID. In: Turcu, C. (ed.) Sustainable Radio Frequency Identification Solutions. Rijeka, Croatia. InTech (2010)
10. Qian, J.-P., et al.: A traceability system incorporating 2D barcode and RFID technology for wheat flour mills. Comput. Electron. Agric. 89, 76–85 (2012). https://doi.org/10.1016/j.compag.2012.08.004
11. Vardhan, G.S., Sivadasan, N., Dutta, A.: QR-code based chipless RFID system for unique identification. 2016 IEEE Int. Conf. RFID Technol. Applicat, 35–39 (2016). https://doi.org/10.1109/RFID-TA.2016.7750744
12. Numan-Al-Mobin, A.M., et al.: RFID integrated QR code tag antenna. 2015 IEEE MTT-S Int. Microw. Symp, 1–3 (2015). https://doi.org/10.1109/MWSYM.2015.7167044
13. Abdelnour, A., Kaddour, D., Tedjini, S.: Transformation of barcode into RFID tag, design, and validation. IEEE Microw. Wireless Compon. Lett. 28(5), 398–400 (2018). https://doi.org/10.1109/lmwc.2018.2822735
14. Online Resource: Sensornation. Accessible: https://sensornation.com/products/sensormatic-a-dr-ultrastrip-labels-iii-barcode-zldrs2-5-000-pcs Last Accessed: 11/01/2022
15. Online Resource: Voyantic Tagformance Pro. Accessible. https://voyantic.com/products/tagformance-pro. Last Accessed: 30 07 2021
16. Colella, R., Chietera, F.P., Catarinucci, L.: Electromagnetic performance evaluation of UHF RFID tags with power discretization error cancellation. IEEE Trans. Antenn. Propag. 67(5), 3545–3549 (2019). https://doi.org/10.1109/tap.2019.2902708
17. Online Resource: GS1 Website. Accessible. https://www.gs1.org/. Last Accessed: 30 07 2021
18. GS1-128 Symbology Specifications, GS1 std. (2006)
19. Liu, B., et al.: An efficient method for antenna design optimization based on evolutionary computation and machine learning techniques. IEEE

Trans. Antenn. Propag. 62(1), 7–18 (2014). https://doi.org/10.1109/tap.2013.2283605
20. Impinj Monza 5 Data Sheet, Impinj, Seattle
21. Dobkin, D.M.: The RF in RFID: Passive UHF RFID in Practice. Elsevier (2007)
22. Yang, L., et al.: RFID tag and RF structures on a paper substrate using inkjet-printing technology. IEEE Trans. Microw. Theor. Tech. 55(12), 2894–2901 (2007). https://doi.org/10.1109/tmtt.2007.909886
23. Virtanen, J., et al.: Inkjet-printed humidity sensor for passive UHF RFID systems. IEEE Trans. Instrum. Meas. 60(8), 2768–2777 (2011). https://doi.org/10.1109/tim.2011.2130070
24. Vena, A., et al.: Design of chipless RFID tags printed on paper by flexography. IEEE Trans. Antenn. Propag. 61(12), 5868–5877 (2013). https://doi.org/10.1109/tap.2013.2281742
25. Catarinucci, L., Colella, R., Tarricone, L.: Prototyping flexible UHF RFID tags through rapid and effective unconventional techniques: validation on label-type sensor-tag. 2012 IEEE Int. Conf. RFID-Technol. Applicat, 176–181 (2012). Nice

How to cite this article: Zannas, K., et al.: Designing UHF RFID tag antennas with Barcode shape for dual-technology identification. IET Microw. Antennas Propag. 16(12), 733–742 (2022). https://doi.org/10.1049/mia2.12269